# Rare gases in lavas from the ultraslow spreading Lena Trough, Arctic Ocean

F. Nauret, Manuel Moreira, J. E. Snow

Geochemistry Geophysics Geosystems G3

*Article*
Volume 11, Number
26 June 2010
Q0AC04, doi:10.1029/2010GC003027
ISSN: 1525-2027

Published by AGU and the Geochemical Society


# Rare gases in lavas from the ultraslow spreading Lena Trough, Arctic Ocean

**F. Nauret**
*Equipe de Géochimie et Cosmochimie, Institut de Physique du Globe de Paris, UMR 7154, Université Paris Diderot, CNRS, 4 place Jussieu, F-75005 Paris, France*

*Max-Planck-Institut für Chemie, Postfach 3060, D-55122 Mainz, Germany*

*Now at Laboratoire Magmas et Volcans, Clermont Université, Université Blaise Pascal, CNRS, IRD, BP 10448, F-63000 Clermont-Ferrand, France (f.nauret@opgc.univ-bpclermont.fr)*

**M. Moreira**
*Equipe de Géochimie et Cosmochimie, Institut de Physique du Globe de Paris, UMR 7154, Université Paris Diderot, CNRS, 4 place Jussieu, F-75005 Paris, France*

**J. E. Snow**
*Max-Planck-Institut für Chemie, Postfach 3060, D-55122 Mainz, Germany*

*Now at Department of Earth and Atmospheric Sciences, University of Houston, Houston, Texas 77204-5007, USA*

[1] Mid-ocean ridge basalts (MORB) from the Arctic Ocean have been much less studied than those from the Indian, Atlantic, and Pacific due to the difficulty of access related to ice cover. In 2001 and 2004 the Arctic ridges (Gakkel Ridge and Lena Trough) were intensively sampled. In this study we present the first helium, neon, and argon concentrations and isotopic ratios in a suite of samples from the ultraslow spreading Lena Trough (~0.75 cm/yr effective full rate). Central Lena Trough (CLT) lavas display $^{4}He/^{3}He$ between 89,710 and 97,530 (R/Ra between 7.4 and 8.1), similar to the mean MORB ratio of 90,000 ± 10,000 (R/Ra = 8 ± 1). In a three neon isotope diagram, the samples fall on the MORB line, without showing any excess of nucleogenic $^{21}Ne$. The $^{40}Ar/^{36}Ar$ ratios vary from 349 to 6964. CLT samples have a typical MORB He and Ne isotopic composition. Rare gases do not indicate any mantle heterogeneities or contribution of subcontinental lithospheric mantle, although this has been suggested previously on the basis of the Sr-Nd and Pb isotopic systems. Based on noble gas systematics, a DUPAL-like anomaly is not observed in the Arctic Ocean. We propose two possible models which reconcile the rare gases with these previous studies. The first is that the Lena Trough mantle has a marble cake structure with small-scale heterogeneities (<1 km), allowing rapid diffusion and homogenization of rare gases compared to elements such as Sr, Nd, and Pb. The second model proposes that the recycled component identified by other isotopic systems was fully degassed at a recent date. It would therefore have a negligible mass budget of rare gases compared to other isotopic systems. This would suggest that the mantle enrichment beneath Lena Trough was generated by rift-forming processes and not by recycling.

**Components:** 7500 words, 5 figures, 2 tables.

**Keywords:** noble gases; MORB; mantle heterogeneity; DUPAL anomaly.

**Index Terms:** 1032 Geochemistry: Mid-oceanic ridge processes (3614); 1038 Geochemistry: Mantle processes (3621); 1025 Geochemistry: Composition of the mantle.

**Received** 4 January 2010; **Revised** 7 May 2010; **Accepted** 17 May 2010; **Published** 26 June 2010.

Nauret, F., M. Moreira, and J. E. Snow (2010), Rare gases in lavas from the ultraslow spreading Lena Trough, Arctic Ocean, *Geochem. Geophys. Geosyst.*, *11*, Q0AC04, doi:10.1029/2010GC003027.

**Theme:** Geochemical Heterogeneities in Oceanic Island Basalt and Mid-ocean Ridge Basalt Sources: Implications for Melting Processes and Mantle Dynamics

## 1. Introduction

[2] Lena Trough is part of the obliquely spreading segment of the North American–Eurasian plate boundary that connects the Knipovitch and Gakkel Ridges (Figure 1). The rifting of Lena Trough began in the Miocene (~10 Ma) [*Crane et al.*, 2001], and is the final and most recent event in the separation of the North American and Eurasian continent. The spreading rate between the two plates in this region is one of the slowest in the world (13 mm full rate, ~7.5 mm/yr effective rate accounting for its 55° obliquity). Lena Trough is considered to be a young nonvolcanic continental rift and details about the geological setting are given elsewhere [*Hellebrand and Snow*, 2003]. Based on Os isotope data obtained from fresh peridotites, the Arctic mantle is depicted as being heterogeneous, composed of refractory and fertile veins in a peridotite matrix [*Liu et al.*, 2008].

[3] During the cruise ARK-XX/2 of the PFS *Polarstern* (Alfred Wegener Institute for Polar and Marine Research, Bremerhaven, Germany) undertaken in the summer of 2004, rare basalts were dredged from the central part of Lena Trough. These basalts (CLT) have been characterized in terms of major-trace elements and Sr-Nd-Pb-Hf isotope systematics (F. Nauret et al., Geochemical composition of Lena Trough lavas (Arctic Ocean), submitted to *Journal of Petrology*, 2010). A Southern Hemisphere DUPAL-like signature is recognized, e.g., radiogenic strontium for low $^{206}Pb/^{204}Pb$ isotopic ratios [*Dupré and Allègre*, 1983; *Hart*, 1984]. Consequently, Lena Trough lavas share similar, but much more extreme, geochemical characteristics with lavas from the westernmost Gakkel Ridge. The latter have been interpreted as reflecting the contribution of ancient Spitzbergen subcontinental lithospheric mantle [*Goldstein et al.*, 2008], which is thought to account for the DUPAL-like nature of many Gakkel Ridge basalts. However, this interpretation seems to be in contradiction with recent Os isotope data obtained from mantle peridotites from Lena Trough, where the contamination by an ancient subcontinental lithospheric mantle (SCLM) component is not observed [*Lassiter and Snow*, 2009]. In order to test for the presence of veins (fertile or refractory) in a mantle source derived from a SCLM or from a deeply recycled component, we have analyzed the noble gas compositions of Lena Trough lavas to constrain the origin of the Southern Hemisphere DUPAL-like geochemical anomaly observed in the Arctic Ocean.

[4] In terms of noble gases, contribution from a SCLM (i.e., R/Ra = 6.1 ± 0.9 [*Gautheron*, 2002]) should provide more radiogenic $^4He/^3He$ isotope ratios for Lena Trough samples compared to samples derived from a mid-ocean ridge basalt (MORB) source (R/Ra = 8 ± 1) [*Day et al.*, 2005; *Gautheron*, 2002]. Similarly, any continental crustal influence or recycled component, such as old oceanic crust ± sediment, might also generate high $^4He/^3He$ isotope ratios and thus R/Ra < 8 ± 1 [*Ballentine and Burnard*, 2002; *Hanyu and Kaneoka*, 1997].

## 2. Sample Descriptions and Analytical Procedures

[5] We measured helium, neon, argon, krypton and xenon concentrations and the He-Ne-Ar isotopic ratios for seven samples from Lena Trough. Samples were glassy rims of basaltic samples from dredges 261 and 262 during the cruise ARK-XX/2 of the PFS *Polarstern*. These lavas have been collected in a geographically restricted area in the central part of Lena Trough (dredge 261: −2.525°E longitude, 80.924°N latitude, depth 3570 m and dredge 262: −2.507°E, 80.907°N latitude, depth 3545 m) and sample 217-1 at the transition zone between Lena Trough and Gakkel Ridge (−6.147°E longitude, 82.857°N latitude). These samples are highly vesicular (up to 25%) despite water depths of over 3500 m (Figure 2) [*Snow et al.*, 2007].

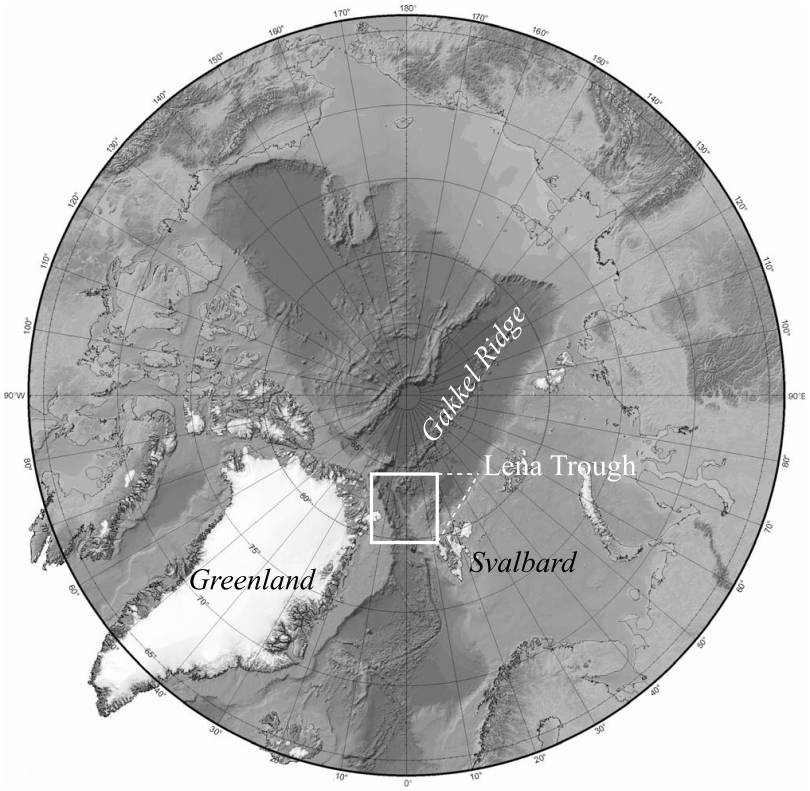


**Figure 1.** Geographical map of the Arctic and North Atlantic oceans where Gakkel Ridge and Svalbard archipelago are reported. The Lena Trough is located in the white square, between Greenland and Svalbard archipelago.

These samples have also been characterized for major and trace elements, and Sr-Nd-Pb-Hf isotopes (Nauret et al., submitted manuscript, 2010).

[6] The analytical procedure is the same as that described by *Moreira et al.* [1995]. Glassy chips were cleaned in deionized water for 15 min in an ultrasonic bath to remove potential contaminants (like seawater or dust, as examples). Cleaned glassy rock chips (1 to 2 g) were loaded in to a crusher and baked overnight at ~150°C under vacuum. The samples were crushed in order to extract the gas. Each step of crushing constituted 15 to 30 strokes. The gas extracted from each step of crushing was purified with two hot Ti getters and a SAES getter at room temperature. The rare gases were trapped at a temperature of 10° K on charcoal using a cryogenic system. Helium was separated from neon at 25° K and neon from the other noble gases at 70 K. Ar, Kr and Xe were desorbed together at 320° K. Rare gases were introduced successively into the ARESIBO II glass mass spectrometer. Typical blanks were $5 \times 10^{-9}$, $4 \times 10^{-13}$ and $2 \times 10^{-12}$ ccSTP for $^{4}$He, $^{22}$Ne and $^{36}$Ar, respectively, with atmospheric isotopic compositions.

## 3. Results

[7] The abundances and isotopic ratios of He, Ne and Ar released by multiple crushing of Lena Trough glasses are given in Tables 1 and 2. Abundances of $^{84}$Kr and $^{130}$Xe are also reported in Table 1. Samples were step crushed between 1 and 3 times. Total $^{4}$He concentrations show a limited range of variation from $1.2 \times 10^{-5}$ to $3.6 \times 10^{-7}$ ccSTP/g, similar to MORB concentrations (Table 1). $^{4}$He/$^{3}$He varies from 89,710 to 97,350 (R/Ra between 7.4 and 8.1 where R is the $^{3}$He/$^{4}$He ratio and Ra the atmospheric ratio: $1.384 \times 10^{-6}$). Helium isotopic ratios are similar to MORB values (90,000 ± 10,000; R/Ra~8 ± 1) (Figure 2). The mean ratio (93,290: R/Ra = 7.75) is similar to Pacific MORB sampled away from hot spots on a ridge with a high spreading rate ($^{4}$He/$^{3}$He = 99,725 ± 2720: R/Ra = 7.3 ± 0.2 [*Moreira et al.*, 2008]). Measured $^{4}$He/$^{3}$He compositions are similar to NMORB reference values and thus slightly more radiogenic compared to MORB from the North Atlantic Ridge (NMAR). So far, MORB from NMAR (Knipovich and Mohns Ridges (72–78°N)) have been described as having high $^{4}$He/$^{3}$He ratios

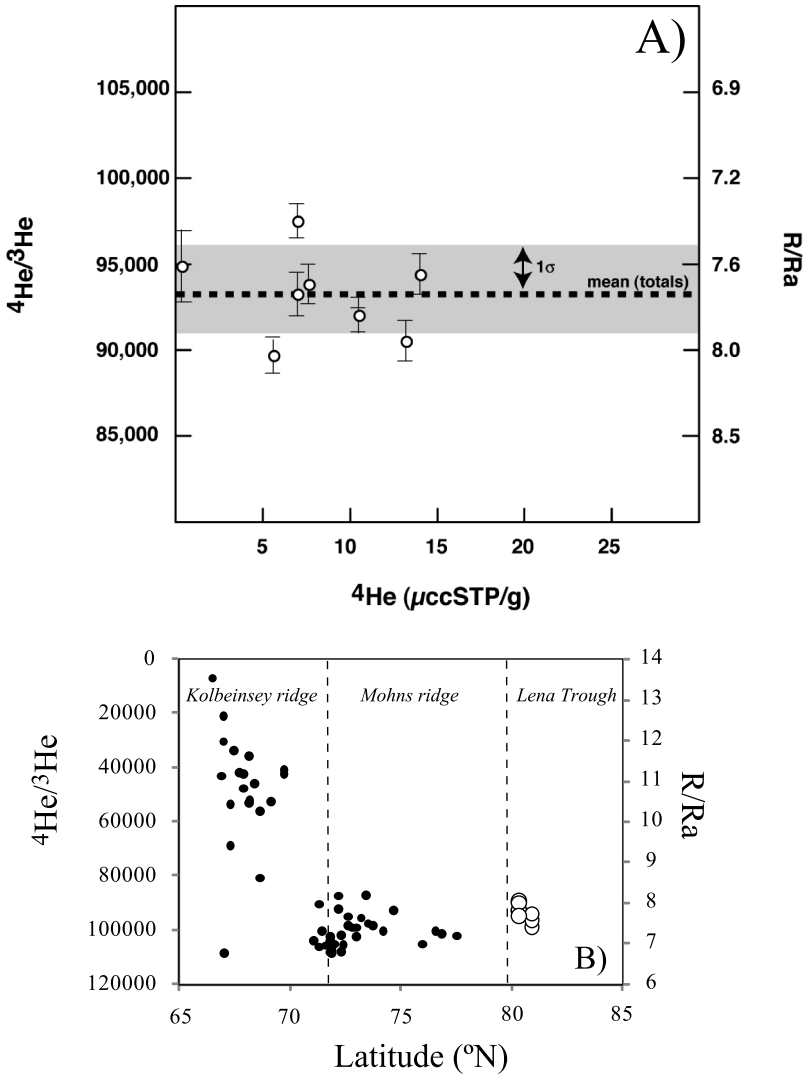


**Figure 2.** (a) Total $^{4}He/^{3}He$ (or R/Ra) versus $^{4}He$. The helium isotopic ratios are very homogeneous compared to other segments from the mid oceanic ridges [*Allègre et al.*, 1995; *Moreira et al.*, 2008]. (b) Comparison between studied samples and MORB from the North Atlantic Ridge [*Macpherson et al.*, 2005; *Schilling et al.*, 1999].

with $^{3}He/^{4}He$ ratios (R/Ra = 6.1–8.1) lower than 8 ± 1 [*Macpherson et al.*, 2005; *Schilling et al.*, 1999] (Figure 2). However, this comparison with MORB from the Knipovich and Mohns Ridges must be treated with caution because helium isotopes can show very large local variations [*Graham*, 2002; *Hilton et al.*, 2000]. Thus, while the samples studied were collected within a geographically restricted area, the MORB samples from the Knipovich and Mohns Ridges cover a distance of more than 1000 km [*Macpherson et al.*, 2005; *Schilling et al.*, 1999].

[8] $^{22}Ne$ concentrations range from $3.1 \times 10^{-10}$ to $1.1 \times 10^{-12}$ ccSTP/g. Neon isotopic ratios vary from 10.08 to 11.04 for $^{20}Ne/^{22}Ne$ and from 0.029 to 0.0434 for $^{21}Ne/^{22}Ne$ (Table 2 and Figure 3). These ratios increase at the second step of crushing relative to the first one (Table 2). At the third step of crushing, $^{20}Ne/^{22}Ne$ and $^{21}Ne/^{22}Ne$ ratios decrease and tend toward atmospheric values but are still higher than values obtained at the first step of crushing (Table 2). Figure 3 shows that the samples fall on the MORB correlation defined by *Sarda et al.* [1988]. The $^{36}Ar$ and $^{40}Ar^{*}$ concentrations (radiogenic argon), $^{40}Ar/^{36}Ar$ and $^{38}Ar/^{36}Ar$ isotopic ratios are reported in Tables 1 and 2. The $^{40}Ar^{*}$ concentrations range over more than 2 orders of magnitude from $6.4 \times 10^{-9}$ to $5.5 \times 10^{-7}$ ccSTP/g. The $^{40}Ar/^{36}Ar$ ratios vary from almost atmospheric (349) to radiogenic ratios of ~7000,

**Table 1.** Depth, Helium, Neon, and Argon Concentrations[a]

| Sample | Depth (m) | Weight (g) | $^{4}$He | $^{22}$Ne | $^{36}$Ar | $^{84}$Kr | $^{130}$Xe | $^{40}$Ar* |
|---|---|---|---|---|---|---|---|---|
| 262-84 step1 | −3545 | 1.26 | 3.04E-06 | 2.96E-10 | 5.66E-09 | 9.52E-11 | 6.11E-13 | 4.59E-07 |
| 262-84 step2 | | | 3.08E-06 | 1.07E-11 | 3.31E-10 | 1.05E-11 | 8.87E-14 | 4.31E-07 |
| 262-84 step3 | | | 8.60E-07 | 5.97E-12 | 1.29E-10 | 3.12E-12 | 7.98E-15 | 1.45E-07 |
| **262-84** | | | **6.98E-06** | **3.12E-10** | **6.12E-09** | **1.09E-10** | **7.07E-13** | **1.04E-06** |
| 262-21 step1 | −3545 | 1.1792 | 4.57E-06 | 1.97E-11 | 8.48E-12 | 2.30E-13 | 1.50E-14 | 7.74E-09 |
| 262-21 step1 | | | 3.06E-06 | 1.02E-11 | 1.48E-12 | 7.20E-14 | 5.80E-15 | 6.39E-09 |
| **262-21** | | | **7.63E-06** | **2.99E-11** | **9.96E-12** | **3.02E-13** | **2.08E-14** | **1.41E-08** |
| 261-1 step1 | −3570 | 1.07 | 7.97E-06 | 5.17E-11 | | | | |
| 261-1 step2 | | | 4.13E-06 | 3.12E-12 | 4.18E-11 | | | 6.43E-08 |
| **261-1** | | | **1.21E-05** | **5.48E-11** | **4.18E-11** | | | **6.43E-08** |
| 261-1B | −3570 | 1.15 | 5.59E-06 | 9.11E-11 | 1.76E-09 | 3.45E-11 | 1.04E-12 | 9.49E-08 |
| 261-1B | | | 4.90E-06 | 4.84E-11 | 9.29E-10 | 1.89E-11 | 6.23E-13 | 9.94E-08 |
| **261-1** | | | **1.05E-05** | **1.40E-10** | **2.69E-09** | **5.34E-11** | **1.66E-12** | **1.94E-07** |
| 261-47 step1 | −3570 | 1.0608 | 3.52E-06 | 4.06E-11 | 1.25E-10 | | | 1.93E-08 |
| 261-47 step1 | | | 2.09E-06 | 1.02E-11 | 1.30E-10 | | | 5.31E-08 |
| **261-47** | | | **5.61E-06** | **5.08E-11** | **2.55E-10** | | | **7.24E-08** |
| 262-34 step1 | −3545 | 1.05 | 4.70E-06 | 2.08E-10 | 4.27E-09 | 8.90E-11 | 3.40E-12 | 5.47E-07 |
| 262-34 step2 | | | 1.97E-06 | 4.46E-12 | 3.66E-11 | 8.90E-13 | 2.30E-14 | 2.44E-07 |
| 262-34 step3 | | | 3.06E-07 | 2.80E-12 | 2.07E-11 | 4.60E-13 | | 9.34E-08 |
| **262-34** | | | **6.98E-06** | **2.15E-10** | **4.33E-09** | **9.04E-11** | **3.42E-12** | **8.84E-07** |
| 261-5 step1 | −3570 | 1.07 | 1.05E-05 | 3.16E-11 | 4.81E-10 | 9.92E-12 | 2.75E-13 | 1.54E-07 |
| 261-5 step2 | | | 2.75E-06 | 4.16E-12 | 1.24E-11 | 9.92E-12 | 2.75E-13 | 3.99E-08 |
| **261-5** | | | **1.32E-05** | **3.57E-11** | **4.93E-10** | **1.98E-11** | **5.51E-13** | **1.94E-07** |
| 261-71 step1 | −3570 | 1.15 | 1.00E-05 | 8.12E-11 | 1.45E-09 | 2.94E-11 | 9.00E-13 | 1.43E-07 |
| 261-71 step2 | | | 3.95E-06 | 5.62E-12 | 6.15E-11 | 1.24E-12 | 6.55E-14 | 5.39E-08 |
| **261-71** | | | **1.40E-05** | **8.68E-11** | **1.51E-09** | **3.06E-11** | **9.66E-13** | **1.97E-07** |
| 217-1 step1 | −4800 | 1.12 | 2.75E-7 | 8.50E-13 | 5.56E-12 | 1.60E-13 | 1.90E-14 | 1.97E-9 |
| 217-1 step2 | | | 8.05E-8 | 2.21E-13 | 7.19E-13 | | | 2.23E-10 |
| **217-1** | | | **3.56E-7** | **1.07E-12** | **6.28E-12** | | | **2.21E-9** |

[a]Concentrations are given in ccSTP/g. Bold values are sums of the amount of gas measured during different steps of crushing.

reflecting mixing between air and a mantle component ($^{40}$Ar/$^{36}$Ar up to 27,000 [*Moreira et al.*, 1998; *Raquin et al.*, 2008]). $^{38}$Ar/$^{36}$Ar ratios are similar to the atmospheric value (0.1880). $^{40}$Ar/$^{36}$Ar ratios increase with the number of steps of crushing (Table 2). Noble gas abundance ratios are also variable. For example, the $^{4}$He/$^{40}$Ar* ratio varies from 3.28 to 590. Note that the mantle production

**Table 2.** Helium, Neon, and Argon Isotope Ratios

| | $^{4}$He/$^{40}$Ar* | σ | $^{4}$He/$^{3}$He | σ | R/Ra | $^{3}$He/$^{22}$Ne | $^{3}$He/$^{22}$Nec | $^{20}$Ne/$^{22}$Ne | σ | $^{21}$Ne/$^{22}$Ne | σ | $^{38}$Ar/$^{36}$Ar | σ | $^{40}$Ar/$^{36}$Ar | σ |
|---|---|---|---|---|---|---|---|---|---|---|---|---|---|---|---|
| 262-84 step1 | 6.6 | 0.6 | 95630 | 1486 | 7.6 | 0.1 | 2.1 | 10.01 | 0.02 | 0.0295 | 0.0003 | 0.1877 | 0.0006 | 377 | 5 |
| 262-84 step2 | 7.1 | 0.6 | 99845 | 1634 | 7.2 | 2.9 | 13.1 | 10.68 | 0.04 | 0.0381 | 0.0007 | 0.1882 | 0.0005 | 1600 | 81 |
| 262-84 step3 | 5.9 | 0.6 | 96315 | 1906 | 7.5 | 1.5 | 12.0 | 10.30 | 0.05 | 0.0346 | 0.0010 | 0.1876 | 0.0005 | 1417 | 89 |
| 262-21 step1 | 590 | 31 | 89881 | 3043 | 8.0 | 2.6 | 15.7 | 10.46 | 0.02 | 0.0360 | 0.0007 | 0.1893 | 0.0007 | 1050 | 6 |
| 262-21 step1 | 479 | 40 | 100487 | 3272 | 7.2 | 3.0 | 11.2 | 10.87 | 0.03 | 0.0422 | 0.0007 | 0.1920 | 0.0013 | 2245 | 30 |
| 261-1 step1 | | | 91579 | 1657 | 7.9 | 1.7 | 37.1 | 9.98 | 0.03 | 0.0311 | 0.0004 | | | | |
| 261-1 step2 | 64.2 | 11.0 | 92469 | 1578 | 7.8 | 14.3 | 35.6 | 11.41 | 0.18 | 0.0491 | 0.0029 | 0.1848 | 0.0011 | 1832 | 251 |
| 261-1B | 58.9 | | 90597 | 1452 | 8.0 | 0.7 | 22.7 | 9.92 | 0.02 | 0.0303 | 0.0005 | 0.1882 | 0.0005 | 349 | 2 |
| 261-1B | 49.3 | | 93777 | 1357 | 7.7 | 1.1 | 31.7 | 9.94 | 0.03 | 0.0302 | 0.0006 | 0.1882 | 0.0004 | 402 | 2 |
| 261-47 step1 | 182 | 10 | 90614 | 2945 | 8.0 | 1.0 | 30.8 | 9.92 | 0.06 | 0.0365 | 0.0040 | 0.1877 | 0.0004 | 451 | 2 |
| 261-47 step1 | 39.4 | 2.1 | 88328 | 3112 | 8.2 | 2.3 | 12.5 | 10.54 | 0.03 | 0.0369 | 0.0006 | 0.1863 | 0.0004 | 707 | 2 |
| 262-34 step1 | 8.6 | 0.5 | 93816 | 1489 | 7.7 | 0.2 | | 9.8 | 0.02 | 0.029 | 0.0003 | 0.1882 | 0.0005 | 424 | 4 |
| 262-34 step2 | 8.1 | 0.4 | 91960 | 2675 | 7.9 | 4.8 | 15.5 | 11.04 | 0.05 | 0.0434 | 0.0008 | 0.1879 | 0.0008 | 6964 | 65 |
| 262-34 step3 | 3.3 | 0.2 | 93290 | 2141 | 7.7 | 1.2 | 6.5 | 10.52 | 0.06 | 0.0385 | 0.0011 | 0.1878 | 0.0005 | 4812 | 46 |
| 261-5 step1 | 68.0 | 3.4 | 90992.11 | 1459.9 | 7.9 | 3.6 | 39.7 | 10.20 | 0.03 | 0.0337 | 0.0004 | 0.1882 | 0.0004 | 616 | 2 |
| 261-5 step2 | 68.9 | 3.5 | 88891.22 | 1339.5 | 8.1 | 7.4 | 39.6 | 10.60 | 0.07 | 0.0388 | 0.0009 | 0.1902 | 0.0006 | 3514 | 37 |
| 261-71 step1 | 70.3 | | 95469.0 | 1551.0 | 7.6 | 1.3 | 23.6 | 10.00 | 0.02 | 0.0311 | 0.0006 | 0.1877 | 0.0004 | 394 | 2 |
| 261-71 step2 | 73.3 | | 91884 | 1478.0 | 7.9 | 7.6 | 32.2 | 10.80 | 0.04 | 0.0396 | 0.0012 | 0.1885 | 0.0004 | 1172 | 7 |
| 217-1 step 1 | 139.6 | 8.0 | 94314 | 2233 | 7.66 | 3.4 | 52.8 | 10.10 | 0.16 | 0.0335 | 0.0020 | 0.1883 | 0.0010 | 651 | 10 |
| 217-1 step 2 | 339.7 | 40 | 97014 | 5059 | 7.45 | 3.8 | 17.1 | 10.68 | 0.44 | 0.0315 | 0.0069 | 0.1870 | 0.0040 | 625 | 35 |

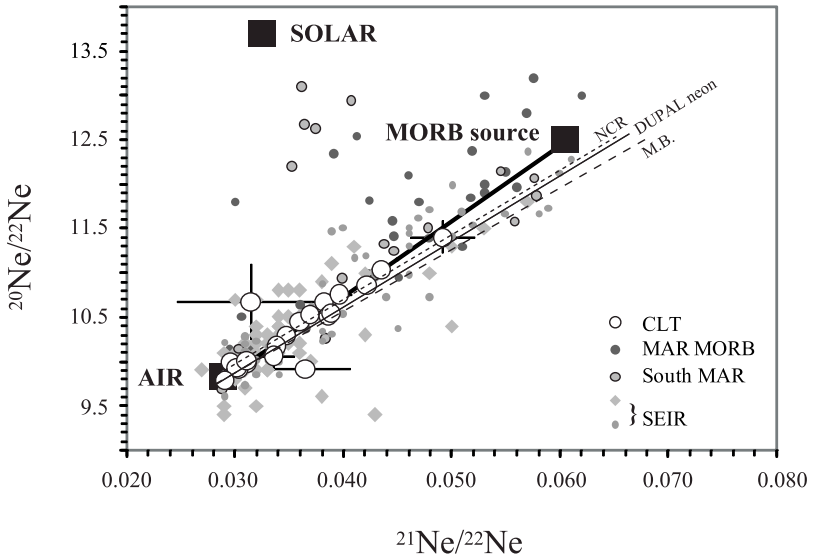


**Figure 3.** Plot of $^{20}Ne/^{22}Ne$ versus $^{21}Ne/^{22}Ne$. Central Lena Trough lavas plot on the MORB reference line defined by *Sarda et al.* [1988], suggesting a binary mixing between DMM and air-like components. Note the extreme homogeneity of the samples. For comparison, we report MORB from the MAR (PetDB database), southern MAR [*Sarda et al.*, 2000], and SEIR [*Burnard et al.*, 2004]. We also show lines defined by the North Chile Ridge [*Niedermann and Bach*, 1998], Manu Basin [*Shaw et al.*, 2001], and DUPAL line estimated from Ne isotope composition of southwest Indian MORB [*Gautheron*, 2002]. Similarly to helium, no DUPAL-like component can be observed for neon (i.e., with nucleogenic neon).

ratio is ~1.8, assuming a K/U of 12,700 [*Jochum et al.*, 1983], or ~1.2 if the MORB source has a K/U of 19,000 [*Arevalo et al.*, 2009]. Total $^{84}Kr$ concentrations range from $7.20 \times 10^{-14}$ to $9.52 \times 10^{-11}$ ccSTP/g. Total $^{130}Xe$ concentrations vary by 3 orders of magnitude from $3.40 \times 10^{-12}$ to $5.80 \times 10^{-15}$ ccSTP/g (Table 1).

## 4. Discussion

### 4.1. Degassing and Initial Gas Content of CLT Magmas

[9] Most $^{4}He/^{40}Ar^*$ ratios in CLT magmas are higher than reasonable production/accumulation values for a MORB source mantle (between 2 and 4 [*Staudacher et al.*, 1989]). Degassing processes are illustrated in Figure 4. In such a diagram, open system degassing (distillation) is represented by straight lines, with a slope of $S_{Ar}/S_{He} - 1$, where $S_{Ar}$ and $S_{He}$ are the solubilities in basalt of argon and helium, respectively. Indeed, during open system degassing, the concentration ratio He/Ar can be written: $\left(\frac{^4He}{^{40}Ar}\right) = \left(\frac{^4He}{^{40}Ar}\right)_0 f^{S_{Ar}/S_{He}-1}$ where $f = {}^{40}Ar/{}^{40}Ar_0$ is the fraction of argon remaining [*Burnard et al.*, 2002; *Moreira and Sarda*, 2000]. $S_{Ar}/S_{He} = 0.105$ according to *Jambon et al.* [1986]. Therefore, in the logarithmic scale diagram of

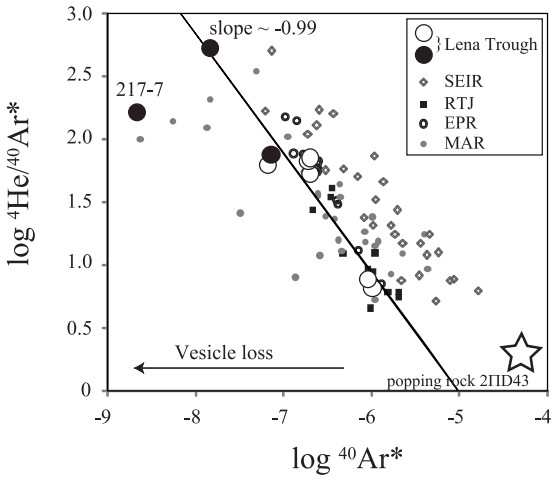


**Figure 4.** Plot of $^{4}He/^{40}Ar$ versus $^{40}Ar^*$. Only totals of the steps of crushing are represented. Data from SEIR [*Burnard et al.*, 2004], MAR [*Sarda et al.*, 2000; *Moreira and Sarda*, 2000], EPR [*Niedermann et al.*, 1997], and the Rodrigues Triple Junction (RTJ) [*Kumagai and Kaneoka*, 2005] are reported for comparison. Data show that the samples may have suffered a distillation-type degassing (slope of −0.99). Since there is no depth variation between the different samples, this degassing can be attributed to major volatile abundance variations. Note the $^{40}Ar^*$ abundance of the highly vesicular popping rock 2πD43 from 14°N in the Atlantic. Black dots are samples that clearly show a distillation process based on Figure 5.

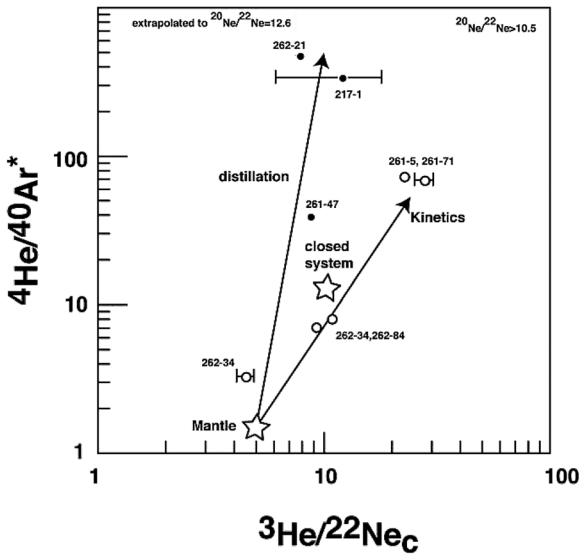


**Figure 5.** Plot of $^{3}He/^{22}Ne_c$ [*Raquin and Moreira*, 2009] versus $^{4}He/^{40}Ar^*$. Only samples with $^{20}Ne/^{22}Ne$ higher than 10.5 are reported. Figure 5 suggests that three samples show a distillation-type degassing (vesiculation in an open system). The other samples indicate a two-step closed system vesiculation loss. Another possible interpretation is that rare gas compositions reflect a vesiculation process with a kinetic effect [*Aubaud et al.*, 2004], suggesting a fast vesiculation during eruption. The calculations were done using the solubilities of *Jambon et al.* [1986]. Mantle ratios are derived from *Moreira et al.* [1998].

Figure 4, distillation processes are straight lines with a slope of ~–0.9. However, the $^{40}Ar$ content is sensitive to vesicle loss after eruption and during sample preparation. This could be the case for sample 217-1, although this sample probably also has a different source composition because it was dredged at a different location. If we exclude this sample, the slope of the regression line is ~–0.99, close to the theoretical value for a distillation process. Therefore, these data could be consistent with a solubility-controlled Rayleigh (fractional) degassing being the dominant fractionating mechanism. However, as mentioned before, such a diagram may not be appropriate in the case of vesicle loss, which certainly occurred in these samples. A complementary diagram is a $^{3}He/^{22}Ne_c$ – $^{4}He/^{40}Ar^*$ diagram, which distinguishes between open system and closed system vesiculation (Figure 5) [*Moreira and Sarda*, 2000; *Sarda et al.*, 2000]. In this diagram, it appears that only three samples clearly suffered an open system vesiculation process (distillation trend, see Figure 5). The others show closed system vesiculation, although possibly with a kinetic effect in order to explain the high $^{3}He/^{22}Ne_c$ ratio [*Aubaud et al.*, 2004]. Therefore, it appears that not all the samples underwent the same degassing process. Some magma vesiculated in a closed system, whereas some vesiculated in an open system. If we consider only the three samples that clearly show a distillation process, it is impossible to derive initial helium or argon concentrations.

[10] Sample 262-34 appears to be the least degassed sample, which appears contrary to its relatively low helium concentration ($7 \times 10^{-6}$ ccSTP/g). Such a helium concentration is relatively low compared to gas-rich popping rocks, which show He contents on the order of a few $10^{-5}$ ccSTP/g and can be considered as undegassed samples [*Javoy and Pineau*, 1991; *Moreira et al.*, 1998; *Sarda and Graham*, 1990; *Staudacher et al.*, 1989]. The low He content of sample 262-34 may reflect vesicle loss during or after eruption.

[11] It is important to note that overall the CLT magmas are not as rich in rare gases as might be expected from a low degree of partial melting (which should result in high noble gas contents) and their high vesicularity (which should indicate high gas contents). This probably reflects vesicle breaking during eruption or sample preparation. Although it is very hard to quantify, we suggest a loss of more than 90% of the vesicles in these samples. Alternatively, the low rare gas concentrations might be linked in a different way to the low degree of partial melting which has generated these Lena Trough lavas. In this scenario, low-degree partial melts are enriched in incompatible elements including $H_2O$. $H_2O$ promotes the formation of the $CO_2$ vapor phase noble gases follow $CO_2$ into this vapor phase, so that an outgassing process during eruption of water-rich magma would result in lavas with lower gas contents when compared to MORB generated by a higher degree of partial melting erupted at similar depth [*Dixon and Stolper*, 1995]. Such relationships have been noted in back-arc lavas, for example from Manus Basin [*Macpherson et al.*, 2005; *Shaw et al.*, 2004].

## 4.2. Mantle Structure and Arctic DUPAL Anomaly

[12] The Lena Trough samples were dredged from a portion of the ridge with an extremely slow spreading rate (~7.5 mm. $yr^{-1}$ effective full rate). Due to the very low magmatic budget along ultraslow spreading ridges, erupted lavas generally display a larger chemical heterogeneity due to the preferential sampling of mantle heterogeneities [*Hirschmann and Stolper*, 1996; *Sinton et al.*, 2002].

These mantle heterogeneities are usually interpreted as reflecting ancient recycled components (e.g., oceanic crust ± sediment, sublithospheric mantle). Therefore, U contained in these recycled components will produce $^4$He by radioactive decay, which results in a high $^4$He/$^3$He. Consequently the $^4$He/$^3$He ratio is a good tracer for the existence of mantle heterogeneities in MORB sources. Mantle heterogeneities have been observed along the Southwest Indian Ridge (SWIR), a slow spreading ridge where $^4$He/$^3$He isotopic ratios are uniformly higher than the MORB value, with $^4$He/$^3$He ratios ranging from 95,000 to 120,000 (R/Ra = 6.0 to 7.6) [*Georgen et al.*, 2003; *Mahoney et al.*, 1989]. Similar high $^4$He/$^3$He isotopic ratios were also clearly identified along the SEIR where the measured R/Ra along the Australian-Antarctic Discordance (AAD) are as low as 6.2 [*Graham*, 2002]. These high $^4$He/$^3$He ratios are classically interpreted as reflecting the presence of recycled crustal or lithospheric material [*Ballentine and Burnard*, 2002; *Graham et al.*, 1992; *Hanyu and Kaneoka*, 1997; *Hilton et al.*, 2000].

[13] The DUPAL anomaly [*Hart*, 1984] is Southern Hemisphere isotopic anomaly whose origin intensively debated in an attempt to identify the nature of recycled components, for example oceanic crust ± sediment, lithospheric mantle, or lower crust [*Escrig et al.*, 2004; *Hanan et al.*, 2004; *Mahoney et al.*, 1992; *Meyzen et al.*, 2005; *Sarda et al.*, 2000]. In terms of noble gases, the DUPAL anomaly is characterized by highly radiogenic He ($^4$He/$^3$He > 120000 [*Gautheron*, 2002] and Ne, mildly radiogenic Ar and atmospheric-like Xe [*Sarda et al.*, 2000]. The origin of the DUPAL material is described by time-integrated, relatively low $^{40}$K/$^{36}$Ar ratios whereas He and Ne suggest elevated (U-Th)/He and (U-Th)/Ne ratios, which could represent lithospheric metasomatized mantle or lower continental crust.

[14] A DUPAL anomaly signature has been recognized on the basis of heavy radiogenic isotopes Sr-Nd-Pb and Hf in the Arctic Ocean [*Goldstein et al.*, 2008; *Mühe et al.*, 1993, 1997] although the $\Delta^{208}$Pb/$^{204}$Pb is less elevated in the Arctic Ocean. Therefore, similar noble gas signatures to those of the Southern Hemisphere DUPAL-like anomaly were expected to be measured in Arctic MORB (along Gakkel ridge and Lena Trough). However, these high $^4$He/$^3$He ratios are not found in our samples. The mean $^4$He/$^3$He ratio in Lena Trough lavas is 93,290 (R/Ra = 7.75). The Lena Trough He isotope ratios ($^4$He/$^3$He = 88,300 to 100,500 or 7.2–8.2 Ra) are less radiogenic than typical values given for Indian MORB with a DUPAL anomaly ($^4$He/$^3$He > 120,000; R/Ra < 6.02) [*Gautheron*, 2002; *Sarda et al.*, 2000] and instead are similar to typical MORB values ($^4$He/$^3$He = 90,000; R/Ra = 8.0). Therefore, the Lena Trough He isotope compositions do not show a typical DUPAL anomaly signature. Moreover, the Lena Trough lavas plot on the MORB line in the three Ne isotope diagrams [*Sarda et al.*, 1988]. The scatter of the data around the MORB line is limited compared to that displayed by SWIR MORB [*Gautheron*, 2002]. Some SWIR MORB values display more radiogenic $^{21}$Ne/$^{22}$Ne at a given $^{20}$Ne/$^{22}$Ne than the MORB reference line (Figure 3). This was interpreted as reflecting the contribution of metasomatized SLCM, which might have generated the Southern Hemisphere DUPAL anomaly [*Gautheron*, 2002]. Alternatively, such high $^{21}$Ne/$^{22}$Ne at a given $^{20}$Ne/$^{22}$Ne is also observed along the North Chile Ridge [*Niedermann and Bach*, 1998] and in the Manus Basin where no SLCM is identified [*Shaw et al.*, 2001] (Figure 3). In these cases, this feature has been interpreted as resulting from a prior melting/degassing event that has fractionated the U/Ne ratio in the residual mantle [*Niedermann and Bach*, 1998; *Shaw et al.*, 2001]. A high $^{21}$Ne/$^{22}$Ne at a given $^{20}$Ne/$^{22}$Ne is not observed in Lena Trough lavas, although a SCLM component might have been expected, taking into account the proximity of the continental margin (80 km away), the Sr-Nd-Pb isotopic composition of MORB from the Arctic Ocean [*Goldstein et al.*, 2008; *Mühe et al.*, 1993, 1997] and the recent opening of the ocean basin in the Lena Trough area.

[15] Thus, taking into account the helium isotopic composition and the data distribution in the three Ne isotope diagram, Lena Trough samples are more like MORB away from a hot spot. A SCLM or previously melted or degassed residual mantle is not observed. In conclusion, the measured He-Ne isotope compositions do not display characteristics shown by the Southern Hemisphere DUPAL signature. Therefore the Southern Hemisphere DUPAL and the Arctic DUPAL-like samples are clearly distinct in terms of noble gas compositions, which indicates a different origin or processes generating this anomaly. This difference between southern and northern DUPAL anomalies could indicate a long-term separation between the two hemispheres [*Jackson et al.*, 2007]. In this case, a mechanism is required to preserve these distinct anomalies since mantle convective stirring tends to attenuate mantle heterogeneities [*van Keken et al.*, 2002]. Alternatively, this difference might be linked to the

abundance, size, relative proportions and variable origins of these mantle heterogeneities [*Meibom and Anderson*, 2004].

[16] Several hypotheses can be formulated to explain the "normal" helium isotope ratio observed at Lena Trough. One is the absence of any mantle heterogeneity, although this goes against the evidence for an enriched, highly potassic mantle source evidenced by the trace element characteristics of the lavas (Nauret et al., submitted manuscript, 2010). A second possibility is that the mantle heterogeneity signal is not recorded in the lavas due to recent gas loss from the enriched component, which then does not, contribute to the noble gas budget during melting. For Hawaii [*Sobolev et al.*, 2005, 2008] a proposed binary melt mixing model involves a melt derived from a MORB source and a melt derived from a second, enriched component, like a SCLM or a recycled component. A similar binary mixing scenario is often proposed for the MAR and Arctic Ridges based on Pb-Pb isotope linear correlations [*Blichert-Toft et al.*, 2005; *Goldstein et al.*, 2008; Nauret et al., submitted manuscript, 2010]. Taking into account, first, that fertile and enriched component melt prior to and deeper than peridotite mantles, and second that this melt might react with surrounding peridotite to form a new pyroxene-rich lithology [*Sobolev et al.*, 2005], it is likely that a melt-vapor fractionation (degassing) occurs during melt formation or melt-rock reaction. Consequently, a melt derived from the enriched component is strongly depleted in volatile elements. Therefore, the signal of the mantle heterogeneity is lost before these two different melts mix to form the sampled lavas. The advantage of this scenario is that it explains the strong decoupling between noble gases and trace element and Sr-Nd-Pb-Hf isotopes which have been interpreted as binary mixing involving more than 50% of enriched component (Nauret et al., submitted manuscript, 2010). The main question in this scenario is why a degassing process occurs at Lena Trough whereas a recycled component in Hawaii or plume derived melts have high $^{3}He/^{4}He$ and $^{20}Ne/^{22}Ne$ for a given $^{21}Ne/^{22}Ne$ [*Coltice and Ricard*, 2002; *Honda et al.*, 1993; *Moreira et al.*, 2001; *Trieloff et al.*, 2000]. As a preliminary answer, we propose that an enriched component melts and forms a volatile incompatible element enriched melt that reacts with the surrounding mantle at a shallow depth than a plume setting. Such shallow depth, low-pressure melting and reaction within Lena Trough mantle allows for melt-vapor fractionation (degassing), which erases the mantle heterogeneity (SCLM or recycled component) signature.

[17] Our preferred explanation is that the mantle heterogeneities (SCLM or veins formed by reaction between a high Si-rich melt derived from a recycled component and peridotite mantle) are volumetrically extremely minor (few $km^3$) and that the helium and neon have been equilibrated by diffusion between the lherzolitic part of the mantle and the recycled component. Therefore the helium and neon isotopic ratios were homogenized, as suggested by *Hart et al.* [2008] for helium. This is possible if the thickness of the heterogeneity is in the order of 1 km and if the time is longer than 1.5 Ga [*Hart et al.*, 2008]. Considering that the lithospheric mantle beneath Svalbard was formed roughly at the same time as the formation of the oldest known crustal rock (up to 2.8 Ga [*Hellman and Witt-Nilsson*, 1999]), we consider our explanation to be a likely scenario. A low melt volume agrees with the observation that no volcanic edifice is observable in bathymetric data.

[18] Lena Trough is thus an example that confirms that spreading rate and noble gas compositions are not related [*Graham*, 2002] and contradicts the hypothesis that slow spreading ridges should have systematically more radiogenic helium compared to faster spreading ridges [*Lupton et al.*, 1993].

## 5. Conclusion

[19] We have reported the first elemental and isotopic compositions of noble gases in lavas collected along the Lena Trough (Arctic Ocean). These lavas appear to have been affected by a strong degassing process, as suggested by the very high $^{4}He/^{40}Ar^{*}$, although they have been collected at great depth (3500 m deep). In contrast to other isotopic systems (Sr-Nd-Pb-Hf), these rare gas compositions do not reflect the presence of long-lived or deep-seated mantle enrichment, which is surprising when taking into account the proximity of the continental margin and the observed geochemical enrichment of the basalts. From the evidence of noble gases, lavas from the Central Lena Trough are generated from a typical MORB source and not from an Arctic DUPAL anomaly. To reconcile the interpretation based on noble gases and radiogenic isotopes, we suggest that mantle heterogeneities are present in the Lena Trough mantle, but their volume are small (<1 km), allowing diffusion of the noble gases, and subsequent homogenization. Another possibility could be that the recycled

component has been degassed and thus plays a minor role in the noble gas mass balance of the Central Lena Trough mantle source.

## Acknowledgments

[20] The authors wish to thank the captain, crew, and other scientific participants in PFS *Polarstern* ARK XX-2 and the Alfred Wegener Institute for access to ship time on PFS *Polarstern*. J.E.S. was supported by grant OCE 0648567 from the National Science foundation and by the Deutsche Forschungsgeminschaft and the Max Planck Society. Thoughtful and thorough reviews by P. Burnard and anonymous reviewer greatly improved the manuscript. This is IPGP contribution 3017.

## References

Allègre, C. J., M. Moreira, and T. Staudacher (1995), $^{4}He/^{3}He$ dispersion and mantle convection, *Geophys. Res. Lett.*, *22*(17), 2325–2328, doi:10.1029/95GL02307.

Arevalo, R., W. F. McDonough, and M. Luong (2009), The K/U ratio of the silicate Earth: Insights into mantle composition, structure and thermal evolution, *Earth Planet. Sci. Lett.*, *278*(3–4), 361–369, doi:10.1016/j.epsl.2008.12.023.

Aubaud, C., F. Pineau, A. Jambon, and M. Javoy (2004), Kinetic disequilibrium of C, He, Ar and carbon isotopes during degassing of mid-ocean ridge basalts, *Earth Planet. Sci. Lett.*, *222*(2), 391–406, doi:10.1016/j.epsl.2004.03.001.

Ballentine, C. J., and P. G. Burnard (2002), Production, release and transport of noble gases in the continental crust, in *Noble Gases in Geochemistry and Cosmochemistry*, *Rev. in Mineral. and Geochem.*, vol. 47, edited by D. Porcelli, C. J. Ballentine, and R. Wieler, pp. 481–538, Mineral. Soc. of Am., Washington, D. C.

Blichert-Toft, J., A. Agranier, M. Andres, R. Kingsley, J.-G. Schilling, and F. Albarède (2005), Geochemical segmentation of the Mid-Atlantic Ridge north of Iceland and ridge–hot spot interaction in the North Atlantic, *Geochem. Geophys. Geosyst.*, *6*, Q01E19, doi:10.1029/2004GC000788.

Burnard, P. G., D. W. Graham, and K. A. Farley (2002), Mechanisms of magmatic gas loss along the Southeast Indian Ridge and the Amsterdam–St. Paul Plateau, *Earth Planet. Sci. Lett.*, *203*(1), 131–148, doi:10.1016/S0012-821X(02)00828-2.

Burnard, P., D. Graham, and K. Farley (2004), Fractionation of noble gases (He, Ar) during MORB mantle melting: A case study on the Southeast Indian Ridge, *Earth Planet. Sci. Lett.*, *227*(3–4), 457–472, doi:10.1016/j.epsl.2004.08.021.

Coltice, N., and Y. Ricard (2002), On the origin of noble gases in mantle plumes, *Philos. Trans. R. Soc. A*, *360*(1800), 2633–2648.

Crane, K., H. Doss, P. Vogt, E. Sundvor, G. Cherkashov, I. Poroshina, and D. Joseph (2001), The role of the Spitsbergen shear zone in determining morphology, segmentation and evolution of the Knipovich Ridge, *Mar. Geophys. Res.*, *22*(3), 153–205, doi:10.1023/A:1012288309435.

Day, J. M. D., D. R. Hilton, D. G. Pearson, C. G. Macpherson, B. A. Kjarsgaard, and P. E. Janney (2005), Absence of a high time-integrated $^{3}He/(U+Th)$ source in the mantle beneath continents, *Geology*, *33*(9), 733–736, doi:10.1130/G21625.1.

Dixon, J. E., and E. M. J. P. Stolper (1995), An experimental study of water and carbon dioxide solubilities in mid-ocean ridge basaltic liquids. 2. Applications to degassing, *J. Petrol.*, *36*(6), 1633–1646.

Dupré, B., and C. J. Allègre (1983), Pb-Sr isotope variation in Indian Ocean basalts and mixing phenomena, *Nature*, *303*(5913), 142–146, doi:10.1038/303142a0.

Escrig, S., F. Capmas, B. Dupre, and C. J. Allègre (2004), Osmium isotopic constraints on the nature of the DUPAL anomaly from Indian mid-ocean-ridge basalts, *Nature*, *431*(7004), 59–63, doi:10.1038/nature02904.

Gautheron, C. (2002), Le manteau lithosphérique sous-continental contraint par la systématique des gaz rares: Apport à la géodynamique chimique des réservoirs terrestres, Ph.D. thesis, 252 pp., Univ. Paris VII, Paris.

Georgen, J. E., M. D. Kurz, H. J. B. Dick, and J. Lin (2003), Low $He^{3}/He^{4}$ ratios in basalt glasses from the western Southwest Indian Ridge (10°–24° E), *Earth Planet. Sci. Lett.*, *206*(3–4), 509–528, doi:10.1016/S0012-821X(02)01106-8.

Goldstein, S. L., G. Soffer, C. H. Langmuir, K. A. Lehnert, D. W. Graham, and P. J. Michael (2008), Origin of a 'Southern Hemisphere' geochemical signature in the Arctic upper mantle, *Nature*, *453*(7191), 89–93, doi:10.1038/nature06919.

Graham, D. W. (2002), Noble gas isotope geochemistry of mid-ocean ridge and ocean island basalts: Characterization of mantle source reservoirs, in *Noble Gases in Geochemistry and Cosmochemistry*, *Rev. in Mineral. and Geochem.*, vol. 47, edited by D. Porcelli, C. J. Ballentine, and R. Wieler, pp. 247–317, Mineral. Soc. of Am., Washington, D. C.

Graham, D. W., W. J. Jenkins, J.-G. Schilling, G. Thompson, M. D. Kurz, and S. E. Humphris (1992), Helium isotope geochemistry of mid-ocean ridge basalts from the South Atlantic, *Earth Planet. Sci. Lett.*, *110*(1–4), 133–147, doi:10.1016/0012-821X(92)90044-V.

Hanan, B. B., J. Blichert-Toft, D. G. Pyle, and D. M. Christie (2004), Contrasting origins of the upper mantle revealed by hafnium and lead isotopes from the Southeast Indian Ridge, *Nature*, *432*(7017), 91–94, doi:10.1038/nature03026. (Corrigendum, *Nature, 432*, 653, doi:10.1038/nature03181, 2004.)

Hanyu, T., and I. Kaneoka (1997), The uniform and low $^{3}He/^{4}He$ ratios of HIMU basalts as evidence for their origin as recycled materials, *Nature*, *390*(6657), 273–276, doi:10.1038/36835.

Hart, S. R. (1984), A large-scale isotope anomaly in the Southern Hemisphere mantle, *Nature*, *309*(5971), 753–757, doi:10.1038/309753a0.

Hart, S. R., M. D. Kurz, and Z. Wang (2008), Scale length of mantle heterogeneities: Constraints from helium diffusion, *Earth Planet. Sci. Lett.*, *269*(3–4), 507–516.

Hellebrand, E., and J. E. Snow (2003), Deep melting and sodic metasomatism underneath the highly oblique-spreading Lena Trough (Arctic Ocean), *Earth Planet. Sci. Lett.*, *216*(3), 283–299, doi:10.1016/S0012-821X(03)00508-9.

Hellman, F., and P. Witt-Nilsson (1999), Single-zircon geochronology of metasediments and a meta-dolerite in the tectonostratigraphy of the Ny Friesland orogen, northeastern Spitsbergen, *J. Conf. Abstr.*, *4*, 594.

Hilton, D. R., C. G. Macpherson, and T. R. G. C. A. Elliott (2000), Helium isotope ratios in mafic phenocrysts and geothermal fluids from La Palma, the Canary Islands (Spain): Implications for HIMU mantle sources, *Geochim. Cosmo-*

*chim. Acta*, *64*(12), 2119–2132, doi:10.1016/S0016-7037(00)00358-6.

Hirschmann, M. M., and E. M. Stolper (1996), A possible role for garnet pyroxenite in the origin of the "garnet signature" in MORB, *Contrib. Mineral. Petrol.*, *124*(2), 185–208, doi:10.1007/s004100050184.

Honda, M., I. McDougall, D. B. Patterson, A. Doulgeris, and D. A. Clague (1993), Noble gases in submarine pillow basalt glasses from Loihi and Kilauea, Hawaii: A solar component in the Earth, *Geochim. Cosmochim. Acta*, *57*(4), 859–874, doi:10.1016/0016-7037(93)90174-U.

Jackson, M. G., M. D. Kurz, S. R. Hart, and R. K. Workman (2007), New Samoan lavas from Ofu Island reveal a hemispherically heterogeneous high $^{3}He/^{4}He$ mantle, *Earth Planet. Sci. Lett.*, *264*(3–4), 360–374, doi:10.1016/j.epsl.2007.09.023.

Jambon, A., H. Weber, and O. G. C. A. Braun (1986), Solubility of He, Ne, Ar, Kr and Xe in a basalt melt in the range 1250–1600°C, *Geochim. Cosmochim. Acta*, *50*(3), 401–408, doi:10.1016/0016-7037(86)90193-6.

Javoy, M., and F. Pineau (1991), The volatiles record of a popping rock from the Mid-Atlantic Ridge at 14°N: Chemical and isotopic composition of gas trapped in the vesicles, *Earth Planet. Sci. Lett.*, *107*(3–4), 598–611, doi:10.1016/0012-821X(91)90104-P.

Jochum, K. P., A. W. Hofmann, E. Ito, H. M. Seufert, and W. M. White (1983), K, U and Th in mid-ocean ridge basalt glasses and heat-production, K/U and K/Rb in the mantle, *Nature*, *306*(5942), 431–436, doi:10.1038/306431a0.

Kumagai, H., and I. G. C. A. Kaneoka (2005), Noble gas signatures around the Rodriguez Triple Junction in the Indian Ocean: Constraints on magma genesis in a ridge system, *Geochim. Cosmochim. Acta*, *69*(23), 5567–5583, doi:10.1016/j.gca.2005.07.013.

Lassiter, J. C., and J. E. G. C. A. Snow (2009), Os-isotope constraints on the origin of Lena Trough peridotites, Arctic Ocean: Asthenospheric mantle or continental lithosphere? *Geochim. Cosmochim. Acta*, *73*(13), A725.

Liu, C. Z., J. E. Snow, E. Hellebrand, G. Brugmann, A. von der Handt, A. Buchl, and A. W. Hofmann (2008), Ancient, highly heterogeneous mantle beneath Gakkel ridge, *Arctic Ocean, Nature*, *452*(7185), 311–316, doi:10.1038/nature06688.

Lupton, J. E., D. W. Graham, J. R. Delaney, and H. P. Johnson (1993), Helium isotope variations in Juan De Fuca Ridge basalts, *Geophys. Res. Lett.*, *20*(17), 1851–1854, doi:10.1029/93GL01271.

Macpherson, C. G., D. R. Hilton, D. F. Mertz, and T. J. G. C. A. Dunai (2005), Sources, degassing, and contamination, of $CO_2$, $H_2O$, He, Ne, and Ar in basaltic glasses from Kolbeinsey Ridge, North Atlantic, *Geochim. Cosmochim. Acta*, *69*(24), 5729–5746, doi:10.1016/j.gca.2005.07.015.

Mahoney, J. J., J. H. Natland, W. M. White, R. Poreda, S. H. Bloomer, R. L. Fisher, and A. N. Baxter (1989), Isotopic and geochemical provinces of the Western Indian Ocean Spreading Centers, *J. Geophys. Res.*, *94*(B4), 4033–4052, doi:10.1029/JB094iB04p04033.

Mahoney, J., A. P. Leroex, Z. Peng, R. L. Fisher, and J. H. Natland (1992), Southwestern limits of Indian Ocean ridge mantle and the origin of low $^{206}Pb/^{204}Pb$ mid-ocean ridge basalt: Isotope systematics of the central Southwest Indian Ridge (17°E–50°E), *J. Geophys. Res.*, *97*(B13), 19,771–19,790, doi:10.1029/92JB01424.

Meibom, A., and D. L. Anderson (2004), The statistical upper mantle assemblage, *Earth Planet. Sci. Lett.*, *217*(1–2), 123–139, doi:10.1016/S0012-821X(03)00573-9.

Meyzen, C. M., J. N. Ludden, E. Humler, B. Luais, M. J. Toplis, C. Mével, and M. Storey (2005), New insights into the origin and distribution of the DUPAL isotope anomaly in the Indian Ocean mantle from MORB of the Southwest Indian Ridge, *Geochem. Geophys. Geosyst.*, *6*, Q11K11, doi:10.1029/2005GC000979.

Moreira, M., and P. Sarda (2000), Noble gas constraints on degassing processes, *Earth Planet. Sci. Lett.*, *176*(3–4), 375–386, doi:10.1016/S0012-821X(00)00010-8.

Moreira, M., T. Staudacher, P. Sarda, J. G. Schilling, and C. J. Allègre (1995), A primitive plume neon component in MORB: The Shona ridge anomaly, South Atlantic (51–52°S), *Earth Planet. Sci. Lett.*, *133*(3–4), 367–377, doi:10.1016/0012-821X(95)00080-V.

Moreira, M., J. Kunz, and C. Allègre (1998), Rare gas systematics in popping rock: Isotopic and elemental compositions in the upper mantle, *Science*, *279*(5354), 1178–1181, doi:10.1126/science.279.5354.1178.

Moreira, M., K. Breddam, J. Curtice, and M. D. Kurz (2001), Solar neon in the Icelandic mantle: New evidence for an undegassed lower mantle, *Earth Planet. Sci. Lett.*, *185*(1–2), 15–23, doi:10.1016/S0012-821X(00)00351-4.

Moreira, M. A., L. Dosso, and H. Ondréas (2008), Helium isotopes on the Pacific-Antarctic ridge (52.5°–41.5°S), *Geophys. Res. Lett.*, *35*, L10306, doi:10.1029/2008GL033286.

Mühe, R., C. W. Devey, and H. Bohrmann (1993), Isotope and trace-element geochemistry of MORB from the Nansen-Gakkel ridge at 86° north, *Earth Planet. Sci. Lett.*, *120*(3–4), 103–109, doi:10.1016/0012-821X(93)90233-Y.

Mühe, R., H. Bohrmann, D. Garbe-Schonberg, and H. Kassens (1997), E-MORB glasses from the Gakkel Ridge (Arctic Ocean) at 87° N: Evidence for the Earth's most northerly volcanic activity, *Earth Planet. Sci. Lett.*, *152*(1–4), 1–9, doi:10.1016/S0012-821X(97)00152-0.

Niedermann, S., and W. Bach (1998), Anomalously nucleogenic neon in North Chile Ridge basalt glasses suggesting a previously degassed mantle source, *Earth Planet. Sci. Lett.*, *160*(3–4), 447–462, doi:10.1016/S0012-821X(98)00103-4.

Niedermann, S., W. Bach, and J. G. C. A. Erzinger (1997), Noble gas evidence for a lower mantle component in MORBs from the southern East Pacific Rise: Decoupling of helium and neon isotope systematics, *Geochim. Cosmochim. Acta*, *61*(13), 2697–2715, doi:10.1016/S0016-7037(97)00102-6.

Raquin, A., and M. Moreira (2009), Atmospheric $Ar^{38}/Ar^{36}$ in the mantle: Implications for the nature of the terrestrial parent bodies, *Earth Planet. Sci. Lett.*, *287*(3–4), 551–558, doi:10.1016/j.epsl.2009.09.003.

Raquin, A., M. A. Moreira, and F. Guillon (2008), He, Ne and Ar systematics in single vesicles: Mantle isotopic ratios and origin of the air component in basaltic glasses, *Earth Planet. Sci. Lett.*, *274*(1–2), 142–150, doi:10.1016/j.epsl.2008.07.007.

Sarda, P., and D. Graham (1990), Mid-ocean ridge popping rocks: Implications for degassing at ridge crests, *Earth Planet. Sci. Lett.*, *97*(3–4), 268–289, doi:10.1016/0012-821X(90)90047-2.

Sarda, P., T. Staudacher, and C. J. Allègre (1988), Neon isotopes in submarine basalts, *Earth Planet. Sci. Lett.*, *91*(1–2), 73–88, doi:10.1016/0012-821X(88)90152-5.

Sarda, P., M. Moreira, T. Staudacher, J. G. Schilling, and C. J. Allègre (2000), Rare gas systematics on the southernmost

Mid-Atlantic Ridge: Constraints on the lower mantle and the Dupal source, *J. Geophys. Res.*, *105*(B3), 5973–5996, doi:10.1029/1999JB900282.

Schilling, J. G., R. Kingsley, D. Fontignie, R. Poreda, and S. Xue (1999), Dispersion of the Jan Mayen and Iceland mantle plumes in the Arctic: A He-Pb-Nd-Sr isotope tracer study of basalts from the Kolbeinsey, Mohns, and Knipovich ridges, *J. Geophys. Res.*, *104*(B5), 10,543–10,569, doi:10.1029/1999JB900057.

Shaw, A. M., D. R. Hilton, C. G. Macpherson, and J. M. Sinton (2001), Nucleogenic neon in high $He^3/He^4$ lavas from the Manus back-arc basin: A new perspective on He-Ne decoupling, *Earth Planet. Sci. Lett.*, *194*(1–2), 53–66, doi:10.1016/S0012-821X(01)00539-8.

Shaw, A. M., D. R. Hilton, C. G. Macpherson, and J. M. G. C. A. Sinton (2004), The $CO_2$-He-Ar-$H_2O$ systematics of the Manus back-arc basin: Resolving source composition from degassing and contamination effects, *Geochim. Cosmochim. Acta*, *68*(8), 1837–1855, doi:10.1016/j.gca.2003.10.015.

Sinton, J., E. Bergmanis, K. Rubin, R. Batiza, T. K. P. Gregg, K. Gronvold, K. C. Macdonald, and S. M. White (2002), Volcanic eruptions on mid-ocean ridges: New evidence from the superfast spreading East Pacific Rise, 17°–19°S, *J. Geophys. Res.*, *107*(B6), 2115, doi:10.1029/2000JB000090.

Snow, J. E., et al. (2007), Petrologic and tectonic evolution of the Lena Trough and Western Gakkel Ridge, *Ber. Polar Meeresforsch., 544*, pp. 153–208, Alfred-Wegener-Inst. für Polar- und Meeresforsch., Bremerhaven, Germany.

Sobolev, A. V., A. W. Hofmann, S. V. Sobolev, and I. K. Nikogosian (2005), An olivine-free mantle source of Hawaiian shield basalts, *Nature*, *434*(7033), 590–597, doi:10.1038/nature03411.

Sobolev, A. V., A. W. Hofmann, G. Brugmann, V. G. Batanova, and D. V. Kuzmin (2008), A quantitative link between recycling and osmium isotopes, *Science*, *321*(5888), 536, doi:10.1126/science.1158452.

Staudacher, T., P. Sarda, S. H. Richardson, C. J. Allègre, I. Sagna, and L. V. Dmitriev (1989), Noble gases in basalt glasses from a Mid-Atlantic Ridge topographic high at 14°N: Geodynamic consequences, *Earth Planet. Sci. Lett.*, *96*(1–2), 119–133, doi:10.1016/0012-821X(89)90127-1.

Trieloff, M., J. Kunz, D. A. Clague, D. Harrison, and C. J. Allègre (2000), The nature of pristine noble gases in mantle plumes, *Science*, *288*(5468), 1036–1038, doi:10.1126/science.288.5468.1036.

van Keken, P. E., E. H. Hauri, and C. J. Ballentine (2002), Mantle mixing: The generation, preservation, and destruction of chemical heterogeneity, *Annu. Rev. Earth Planet. Sci.*, *30*, 493–525, doi:10.1146/annurev.earth.30.091201.141236.